Ring Currents and Aromaticity of Monocyclic π-Electron Systems C_6H_6, $B_3N_3H_6$, $B_3O_3H_3$, $C_3N_3H_3$, $C_5H_5^-$, $C_7H_7^+$, $C_3N_3F_3$, $C_6H_3F_3$, and C_6F_6

Patrick W. Fowler* and Erich Steiner

Department of Chemistry, University of Exeter, Stocker Road, Exeter EX4 4QD, U.K.

Received: November 13, 1996[⊗]

A distributed-origin coupled Hartree−Fock method is used to compute and map the π and total current densities induced by a magnetic field in the planar monocyclic molecules benzene (C_6H_6), borazine ($B_3N_3H_6$), boroxine ($B_3O_3H_3$), *s*-triazine ($C_3N_3H_3$), the cyclopentadienyl anion ($C_5H_5^-$), and the tropylium cation ($C_7H_7^+$). The maps show that *s*-triazine, the cyclopentadienyl anion, and the tropylium cation have delocalized π ring currents similar to that in benzene whereas the π currents are localized on the nitrogens in borazine and on the oxygens in boroxine. The computed magnetic susceptibilities show trends that follow those observed for the ring currents and provide measures of the "aromaticity" of the molecules. Current density maps of the symmetric trifluorides of benzene ($C_6H_3F_3$) and triazine ($C_3N_3F_3$) and of perfluorobenzene (C_6F_6) show independent localized circulations of π charge on the fluorines with a weak compression of the region of circulation in the ring.

Introduction

The concept of ring currents as properties of the π electrons in monocyclic (and polycyclic) conjugated systems is widely used by chemists as an interpretative tool in nuclear magnetic resonance spectroscopy.[1−5] One manifestation of ring currents is the low-field chemical shift in the proton NMR spectrum of benzene and other conjugated systems. Another is the marked anisotropy of the magnetic susceptibility in such systems, with the component of magnetizability in the direction perpendicular to the molecular plane much larger (more than twice as large in benzene) than that in directions parallel to the plane. It is only through such manifestations that the existence and behavior of ring currents can be inferred. However, although they are not directly observable, ring currents can nevertheless be obtained from theory by computing the response of a molecular system to an applied magnetic field. The efficacy of recently developed distributed gauge methods of computing ring currents and other magnetic properties has been demonstrated for benzene and for several other conjugated systems.[6−14] The current maps of benzene, for example, show the diamagnetic circulation of π electrons around the carbon ring that has been popularly anticipated and that has become almost a hallmark of the π-electron delocalization associated with the aromaticity of the molecule. The maps for naphthalene, anthracene, and other polyacenes also show π currents that span some or all of the carbon rings,[15] and they support the interpretation of trends in the chemical and physical properties of this series of molecules in terms of a decline in "aromatic character" as the length of the molecule is increased.[16−18]

The present work is concerned with *ab initio* computations of magnetic properties, including ring currents, of a number of planar monocyclic systems. The molecules discussed are benzene (C_6H_6) and its inorganic analogues borazine ($B_3N_3H_6$) and boroxine ($B_3O_3H_3$), often referred to as "inorganic benzenes" [*e.g.*, refs 19−21]; also *s*-triazine ($C_3N_3H_3$) which, like borazine and boroxine, is isoelectronic with benzene, and the cyclopentadienyl anion ($C_5H_5^-$) and tropylium cation ($C_7H_7^+$) which, as systems with six π electrons, are often discussed in conjunction with benzene in introductions to Hückel and other π-electron theories. The numerical results of these computations are presented in Tables 1−3 and the current density maps in Figures 1−6. In addition, computations of the magnetic properties of the symmetric trifluorides of benzene ($C_6H_3F_3$) and triazine ($C_3N_3F_3$) and for perfluorobenzene (C_6F_6) have been performed to study the effect on the ring currents of substituting fluorine for hydrogen. The relevant current density maps (Figures 7−9) are presented in this paper.

Kutzelnigg and co-workers[14] have already performed a careful analysis of the magnetic properties of benzene and some of its isomers. Our results for the magnetic susceptibility are in close agreement with that work, and we have equal confidence in the quality of the results for the other systems considered here. We find, in these systems also, that the component of the susceptibility, $\chi_{\parallel}$, parallel to the principal axis (perpendicular to the molecular plane) can be used as a measure of aromaticity. There exists a vast literature on the definition of aromaticity and on the interpretation of aromaticity in terms of a variety of observed and derived properties of conjugated systems, of which the most prominent are aromatic stabilization energy and magnetic susceptibility exaltation.[17,18,22,23] Schleyer *et al.*[23] state "*Despite the fundamental importance of aromaticity and antiaromaticity in chemistry, no generally acceptable definition has been established*". These authors suggest that aromaticity of the five-membered C_4H_4X ring systems is effectively characterized by the combination of a number of geometric, energetic, and magnetic parameters. A recent review of the relative merits of the parameters by Schleyer and Jiao[24] concludes, however, that diamagnetic susceptibility exaltation[25] may be the unique criterion for aromaticity. Most recently, Schleyer *et al.*[26] have proposed the use of absolute magnetic shieldings computed at ring centers as a new aromaticity/antiaromaticity criterion that is less dependent on the size of the system and, therefore, particularly useful for multi-ring systems.

Kutzelnigg *et al.*[14] state "*We think that it is now time to come to a definite conclusion* [as to the ring current model], *since the theoretical methods available should make this possible*". It is the principal purpose of the present work to show that electron current density maps can shed new light on the meaning of the numbers and, at least for the six-membered ring systems

[⊗] Abstract published in *Advance ACS Abstracts,* January 15, 1997.

S1089-5639(96)03794-2 CCC: $14.00

considered here, can give an unambiguous answer to the question, "Is the molecule aromatic?"

Method

The magnetic properties of the title molecules in their closed-shell ground states were computed within the oribital approximation by the coupled Hartree−Fock (CHF) method using the SYSMO package of programs.[27] It is well-known that[28] whereas exact solution of the CHF equations gives magnetic properties that are independent of the choice of gauge origin (the origin of the vector potential of the external magnetic field), this independence is not preserved for approximate solutions. Different choices of gauge origin may be appropriate for different properties; for example, the electronic centroid for magnetizability[29] or a computationally determined point that is often close to the nearest heavy nucleus for nuclear shielding.[30] Several schemes that have been proposed for the calculation of magnetic properties use multiple gauge centers. Examples are Kutzelnigg's IGLO approach,[12,13] which defines the centers in terms of localized molecular orbitals, and London's GIAO method,[2,31,32] which associates a gauge factor with each basis function.

In the present work, the magnetizability tensor χ was computed with gauge origin at the geometric center of each molecule. The current density vector field **j**(**r**), however, was computed using the continuous gauge formulation denoted by the acronym CGTR (for continuous gauge transformation) by Keith and Bader[6] and by CTOCD-DZ (for continuous transformation of origin of current density with diamagnetic current set to zero) by Lazzeretti *et al.*[8−11] In this formulation the current density **j**(**r**) at each point **r** is computed with that point as gauge origin. One consequence of this choice of gauge distribution is that the diamagnetic component of **j**(**r**) that describes the classical circulation of charge about the (single) gauge origin is formally set to zero, being replaced by a term that depends on the first-order wave function obtained by treating the linear momentum operator as a perturbation. The more significant practical consequence is that this choice is known to give realistic current densities with even quite small basis sets.[6,10,15] With the basis sets used in the present work, **j**(**r**) is close to the CHF limiting value except at points close to the nuclei, where the density is underestimated.

The calculations of properties were performed with the MODENA III basis sets of Lazzeretti *et al.*[19,33] These are Cartesian contracted Gaussian basis sets (13s8p2d) → [8s6p2d] for atoms B to F and (8s2p) → [6s2p] for hydrogen. The (13s8p) sets for atoms B to F and the (8s) set for hydrogen are taken from the compilation of van Duijneveldt.[34] The two uncontracted polarization functions for each atom are obtained by decontraction of the two Gaussian representations of single Slater-type orbitals (STO) obtained with Dunning's prescription.[35] The exponent of the p-type STO for H is 1.24; the exponents of the d-type STO are 1.87 for B, 1.78 for C, 1.80 for N, and 1.93 for O. The corresponding exponent for F has been taken as 2.0. The exponents of the Gaussian polarization functions are 0.8566 and 0.1993 for H, 1.1433 and 0.3387 for B, 1.0367 and 0.3071 for C, 1.0602 and 0.3140 for N, 1.2188 and 0.3610 for O, and 1.3088 and 0.3877 for F. The molecular geometries of all the systems were obtained in a systematic way by optimization at the SCF level with the 6-31G** basis using the CADPAC package.[36] The use of bigger basis sets and of higher levels of theory leads to geometries a little different from those used here but to no significant changes to the properties presented in this paper.

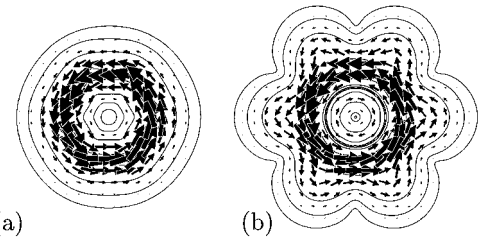

Figure 1. Current density maps in benzene (C_6H_6): (a) π current; (b) total ($\sigma + \pi$) current. The maps show the current density field **j** in a plane 1 bohr above the molecular plane. The plotting area is a square of side 16 a_0. The contours show the modulus of the complete current density, $|\mathbf{j}|$, with contour values of 0.001×4^n au, for $n = 0, 1, 2, ...$ The vectors (arrows) are centered on the points of a 24×24 grid and show the magnitude and the direction of the projection of **j** in the plane.

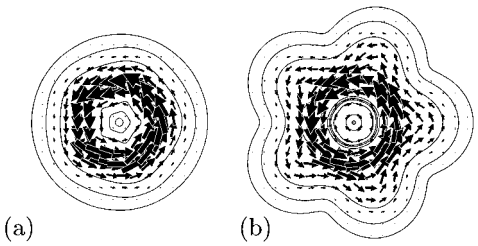

Figure 2. Current density maps in the cyclopentadienyl anion ($C_5H_5^-$): (a) π current; (b) total ($\sigma + \pi$) current. Details are as for Figure 1.

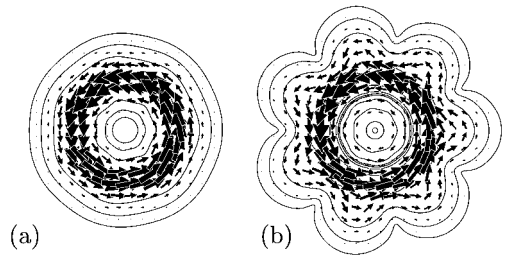

Figure 3. Current density maps in the tropylium cation ($C_7H_7^+$): (a) π current; (b) total ($\sigma + \pi$) current. Details are as for Figure 1.

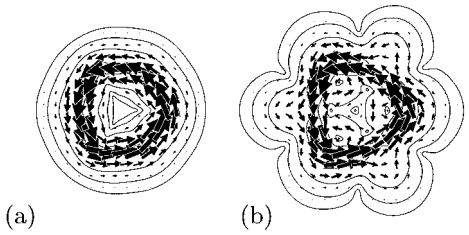

Figure 4. Current density maps in *s*-triazine ($C_3N_3H_3$): (a) π current; (b) total ($\sigma + \pi$) current. Details are as for Figure 1.

Current Density Maps

The current densities induced by a magnetic field of unit strength perpendicular to the molecular plane in benzene and its analogues are shown in Figures 1−6. The current densities in these figures (and in Figures 7−9) have been computed in a plane parallel to and at distance 1 a_0 from the plane of the nuclei. This choice of vertical displacement arose from (unpublished) numerical experiments for benzene that showed that the resulting reference plane is close to that of maximum π current density and that the computed currents in this plane (for benzene) are almost identical in the single- and continuous-gauge formulations with the MODENA III basis. At this height the flow is essentially parallel to the molecular plane so that no significant error is introduced by neglecting the component of **j** parallel to the inducing field. All the figures are drawn to the same scale. For each system, map a is the π current and map b is the total

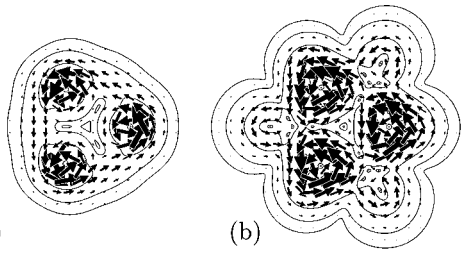

Figure 5. Current density maps in borazine ($B_3N_3H_6$): (a) π current; (b) total ($\sigma + \pi$) current. Details are as for Figure 1.

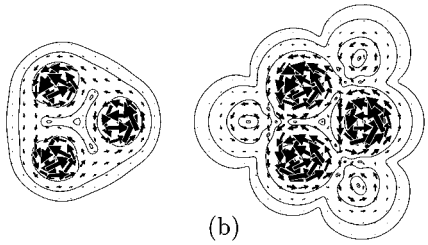

Figure 6. Current density maps in boroxine ($B_3O_3H_3$): (a) π current; (b) total ($\sigma + \pi$) current. Details are as for Figure 1.

TABLE 1: Largest Current Densities j_{max} (au) Computed in the CTOCD-DZ Formulation with the MODENA III Basis in a Plane 1 bohr above the Molecular Plane

	(a) π current	(b) total current	(a)/(b)
1. benzene (C_6H_6)	0.077	0.101	0.76
2. cyclopentadienyl ($C_5H_5^-$)	0.070	0.096	0.73
3. tropylium ($C_7H_7^+$)	0.080	0.103	0.78
4. *s*-triazine ($C_3N_3H_3$)	0.078	0.111	0.70
5. borazine ($B_3N_3H_6$)	0.044	0.076	0.58
6. boroxine ($B_3O_3H_3$)	0.050	0.092	0.54
7. trifluorotriazine ($C_3N_3F_3$)	0.062	0.094	0.66
8. trifluorobenzene ($C_6H_3F_3$)	0.078	0.089	0.88
9. hexafluorobenzene (C_6F_6)	0.080	0.091	0.88

($\sigma + \pi$) current. The plotting area is a square of side 16 a_0. The contours show the modulus of the complete current density, $|\mathbf{j}|$, with contour values 0.001×4^n au, for $n = 0, 1, 2, ...$ The vectors (arrows) are centered on the points of a 24×24 grid and show the magnitude and the direction of the projection of **j** in the plane. The magnitudes, j_{max}, of the largest computed density in our chosen reference plane (computed on a 500×500 grid) are listed in Table 1.

The maps demonstrate a very clear distinction between the π currents (and the total currents) in C_6H_6, $C_5H_5^-$, $C_7H_7^+$, and $C_3N_3H_3$ (Figures 1−4) and those in the inappropriately named "inorganic benzenes" borazine and boroxine (Figures 5 and 6). In each of the former there is a simple (diamagnetic) circulation of π charge with maximum density on (that is, above and below) the atoms of the ring. In borazine and boroxine, however, the π current consists of three islands of circulation localized on the nitrogens in borazine and on the oxygens in boroxine. The values of j_{max} in Table 1 show that this localization is accompanied by a decrease in both the strength of the π current, at 1 bohr above the molecular plane, and in the ratio of π-to-total current strength in this plane.

The current density maps in Figures 1−6 demonstrate a trend that is consistent with the variation of extent of aromaticity, or of π-charge delocalization, in the expected decreasing order: benzene, *s*-triazine, borazine, boroxine. The same trend has been deduced from other studies; for example, from resonance energies,[37] from plots of the Laplacian of the probability density, $\nabla^2\rho(\mathbf{r})$,[38] and from plots of the localized orbitals calculated in spin-coupled valence-bond theory.[20]

The current density maps of the trifluorides of triazine and benzene and for hexafluorobenzene are displayed in Figures 7−9; they are drawn to the same scale as in Figures 1−6. Their most striking features are the independent localized circulations of π charge on the fluorines with a weak compression of the region of circulation in the ring. A comparison of Figures 4 and 7 shows that the strength of current in the ring of triazine, at 1 bohr above the molecular plane, is decreased on substitution of hydrogen by fluorine, and this is confirmed in Table 1 by the corresponding decrease in j_{max} values. There is little change, however, in the strength of the π current of the benzene ring on substitution.

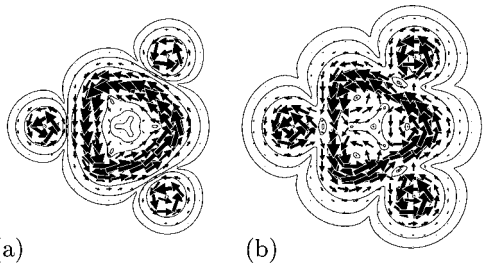

Figure 7. Current density maps in *s*-trifluorotriazine ($C_3N_3F_3$): (a) π current; (b) total ($\sigma + \pi$) current. The maps show the current density field **j** in a plane 1 bohr above the molecular plane. The plotting area is a square of side 18 a_0. The contours show the modulus of the complete current density, $|\mathbf{j}|$, with contour values of 0.001×4^n au, for $n = 0, 1, 2, ...$ The vectors (arrows) are centered on the points of a 24×24 grid and show the magnitude and the direction of the projection of **j** in the plane.

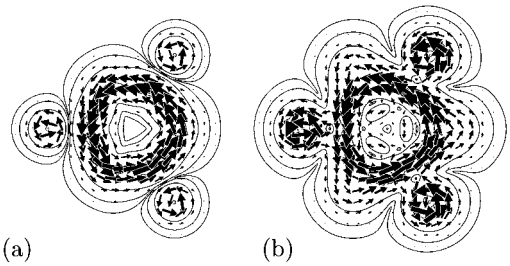

Figure 8. Current density maps in *s*-trifluorobenzene ($C_6H_3F_3$): (a) π current; (b) total ($\sigma + \pi$) current. Details are as for Figure 7.

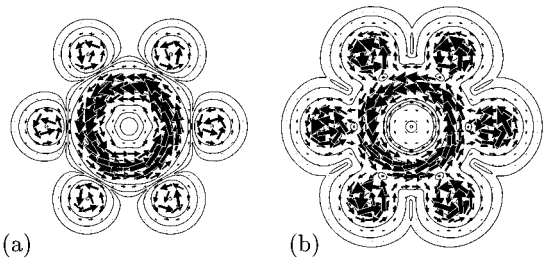

Figure 9. Current density maps in hexafluorobenzene (C_6F_6): (a) π current; (b) total ($\sigma + \pi$) current. Details are as for Figure 7.

Magnetic Susceptibility and an Aromaticity Scale

The trend observed pictorially in the current density maps of benzene and its analogues is quantified in the tabulation of the corresponding computed molecular magnetic susceptibilities (magnetizabilities) in Table 2. The most notable feature of the results is that the large anisotropy, $\Delta\chi = \chi_{\parallel} - \chi_{\perp}$, in the susceptibility of the "aromatic" molecules arises mainly from the large anisotropy for the π electrons. The component $\chi_{\parallel}$ in the direction parallel to the principal axis of the molecule (perpendicular to the molecular plane) is a measure of freedom of circulation in the presence of a magnetic field in this direction. For benzene, the archetypal aromatic molecule, the value of this component is −11.3 au or −1.9 au per π electron. The ratio $\chi_{\parallel}/\chi_{\parallel}(C_6H_6)$ for another, similar molecule can then

TABLE 2: Computed Magnetic Susceptibilities of Benzene, Cyclopentadienyl Anion, Tropylium cation, *s*-Triazine, Borazine, and Boroxine[a]

	C_6H_6[b]	$C_5H_5^-$	$C_7H_7^+$	$C_3N_3H_3$	$B_3N_3H_6$	$B_3O_3H_3$
			inner shell			
$\chi_\perp$	−0.8176	−0.5857	−1.1034	−0.7756	−0.8944	−0.8765
$\chi_\parallel$	−2.0427	−1.2406	−3.1084	−1.8050	−2.0945	−1.9175
$\bar{\chi}$	−1.2259	−0.8040	−1.7717	−1.1187	−1.2945	−1.2235
$\Delta\chi$	−1.2251	−0.6549	−2.0050	−1.0294	−1.2001	−1.0410
			valence σ			
$\chi_\perp$	−7.2193	−8.0087	−6.7987	−5.1516	−8.9920	−7.8855
$\chi_\parallel$	−9.8054	−9.9223	−10.5542	−7.2137	−9.2060	−7.1633
$\bar{\chi}$	−8.0813	−8.6465	−8.0504	−5.8390	−9.0633	−7.6447
$\Delta\chi$	−2.5861	−1.2389	−3.7555	−2.0621	−0.2140	+0.7222
			valence π			
$\chi_\perp$	−0.7686	−0.9272	−0.1424	−0.0989	−0.5023	−0.0477
$\chi_\parallel$	−11.2859	−9.7805	−13.9203	−7.9481	−3.7560	−2.3525
$\bar{\chi}$	−4.2744	−3.8783	−4.7350	−2.7153	−1.5869	−0.8160
$\Delta\chi$	−10.5173	−8.8533	−13.4963	−7.8492	−3.2537	−2.3008
$\chi_\parallel/\chi_\parallel(C_6H_6)$	1.000	0.867	1.233	0.704	0.333	0.208
$\Delta\chi/\Delta\chi(C_6H_6)$	1.000	0.842	1.283	0.746	0.309	0.219
			total			
$\chi_\perp$	−8.8054	−9.5215	−8.0445	−6.0262	−10.3887	−8.8096
$\chi_\parallel$	−23.1340	−20.9434	−27.5825	−16.9668	−15.0564	−11.4332
$\bar{\chi}$	−13.5816	−13.3288	−14.5572	−9.6730	−11.9446	−9.6842
$\Delta\chi = \chi_\parallel - \chi_\perp$	−14.3286	−11.4219	−19.5380	−10.9406	−4.6677	−2.6236
$\Delta\chi/\Delta\chi(C_6H_6)$	1.000	0.797	1.364	0.764	0.326	0.184

[a] Susceptibilities are given in atomic units: 1 au $= e^2a_0^2/m_e = 7.891\,04 \times 10^{-29}$ J T$^{-2} \equiv 4.752\,09 \times 10^{-6}$ cgs emu. [b] The small differences between the values listed here and those computed with the same basis set by Lazzeretti *et al.*[33] are due to the use of different molecular geometries.

plausibly be regarded as a measure of its aromaticity (relative to benzene). The values of this ratio given in Table 2 then represent an "aromaticity scale" that parallels the trend observed in the current density maps. In particular, the values of these computed aromaticity indices confirm the distinction between C_6H_6, $C_5H_5^-$, $C_7H_7^+$ and $C_3N_3H_3$ on the one hand, with "large" values, and borazine and boroxine on the other, with much smaller values. The order in the computed scale of aromaticity is

$$C_7H_7^+ > C_6H_6 > C_5H_5^- > C_3N_3H_3 > B_3N_3H_6 > B_3O_3H_3$$

This is the expected order for the neutral species, but the positions of the ions are problematic both because of the charges and because of the different sizes of ring. The negative charge and smaller ring of the cyclopentadienyl anion may be expected to be opposed in their effects on the susceptibility, as may the positive charge and larger ring size of the tropylium cation. Calculations of diamagnetic susceptibility exaltations support our result that $C_7H_7^+$ is "more aromatic" than C_6H_6, with typical exaltation values (in units 10^{-6} cgs emu) of (a) −13.7 for C_6H_6 and −17.0 for $C_7H_7^+$ (ratio 1.24)[25] and (b) −13.4 for C_6H_6 and −20.5 for $C_7H_7^+$ (ratio 1.53)[26]. On the other hand, the computed nucleus-independent chemical shift (NICS) values (in ppm) of −9.7 for C_6H_6 and −7.6 for $C_7H_7^+$ (ratio 0.78) suggest the opposite.[26] Both the exaltation and NICS indices put the cyclopentadienyl anion above benzene in the scale, with ratios 1.28 and 1.47, respectively,[26] whereas our computed anisotropy puts it below.

Table 2 shows that for the π electrons the components $\chi_\perp$ in the plane of the molecules are much smaller than the corresponding components $\chi_\parallel$ perpendicular to the plane, even in borazine and boroxine. It follows that aromaticity indices obtained from the anisotropies $\Delta\chi$ for the π electrons are almost identical to those obtained from $\chi_\parallel$. This is of course not necessarily true for other sequences of molecules. For example, a completely different pattern of behavior is exhibited by the isoelectronic family of triangular 2π-electron systems of which the cyclopropenyl cation $C_3H_3^+$ is a typical member.[39] Table 2 also shows that the inner-shell and valence σ electrons make significant contributions not only to the total average susceptibilities but also to the anisotropies. Such contributions to magnetic (and other) properties have been interpreted as "local", in contrast to "nonlocal" contributions from delocalized π electrons (see ref 14 for a recent discussion of such interpretations, with particular reference to benzene), but in some molecules it is the valence σ electrons that may need to be considered as providing the nonlocal contributions.[39] For the conjugated systems discussed here, however, the contributions of the inner-shell and valence σ electrons to the anisotropies are sufficiently small for the *total* anisotropies to give a pattern of aromaticity indices almost identical to that obtained from the π electrons alone. Experimental values of total susceptibilities and total anisotropies are $\bar{\chi} = -11.5$ au, $\Delta\chi = -13.1$ au for benzene,[40] $\bar{\chi} = -8.0$ au, $\Delta\chi = -8.0$ au for *s*-triazine,[41] and $\bar{\chi} = -10.4$ au, $\Delta\chi = -5.4$ au for borazine.[40] The corresponding values of $\Delta\chi/\Delta\chi(C_6H_6)$ are 0.61 and 0.41 for *s*-triazine and borazine, respectively, and there are not too far from the computed values given in the last line of Table 2 for these molecules.

We have also computed ring currents and properties of pyridine and pyrrole with the MODENA III basis. The computed current density maps (not shown here) exhibit typical aromatic behavior, pyridine having a π ring current similar to that of benzene and pyrrole with ring current similar to that in cyclopentadienyl. The aromaticity indices of pyridine and pyrrole on the three scales described above are 0.92, 0.94, and 0.95 for pyridine and 0.66, 0.67, and 0.66 for pyrrole.

An alternative measure of the freedom of movement of π electrons in a planar conjugated system is given by the components of the electric dipole polarizability in the plane.[19,21] The computed polarizabilities are given in Table 3. Experimental values of the mean total polarizability $\bar{\alpha}$ are 67.5 au for benzene[42] and 59.7 au for borazine,[43] providing some confidence in the accuracy of the computed values. Experimental values of the total polarizability anisotropy $\Delta\alpha$ are (in au) 35.0

TABLE 3: Computed Electric Dipole Polarizabilities of Benzene, Cyclopentadienyl Anion, Tropylium Cation, *s*-Triazine, Borazine, and Boroxine[a]

	C_6H_6[b]	$C_5H_5^-$	$C_7H_7^+$	$C_3N_3H_3$	$B_3N_3H_6$	$B_3O_3H_3$
			inner shell			
$\alpha_\perp$	0.0363	0.0309	0.0407	0.0319	0.0701	0.0688
$\alpha_\parallel$	0.0128	0.0152	0.0124	0.0056	0.0115	0.0072
$\bar{\alpha}$	0.0285	0.0257	0.0312	0.0231	0.0506	0.0483
			valence σ			
$\alpha_\perp$	35.9575	33.3996	37.0049	29.2445	41.2225	32.6943
$\alpha_\parallel$	13.2929	10.4035	15.8535	13.8217	18.6290	18.3343
$\bar{\alpha}$	27.7360	25.7343	29.9544	24.1036	33.6914	27.9076
$\Delta\alpha$	22.6646	22.9961	21.1514	15.4226	22.5935	14.3600
			valence π			
$\alpha_\perp$	42.2259	44.4522	52.1687	26.7943	21.0788	11.0652
$\alpha_\parallel$	30.1645	43.5126	26.0867	17.3294	21.8528	11.6705
$\bar{\alpha}$	38.2054	44.1390	43.4747	23.6393	21.3368	11.2670
$\Delta\alpha$	12.0614	0.9396	26.0820	9.4649	−0.7740	−0.6053
$\alpha_\perp/\alpha_\perp(C_6H_6)$	1.000	1.053	1.235	0.635	0.499	0.262
$\Delta\alpha/\Delta\alpha(C_6H_6)$	1.000	0.078	2.162	0.785	−0.064	−0.050
			total			
$\alpha_\perp$	77.2197	77.8827	89.2142	56.0707	62.3715	43.8283
$\alpha_\parallel$	43.4702	53.9313	41.9526	31.1567	40.4934	30.0120
$\bar{\alpha}$	65.9699	69.8989	73.4603	47.7660	55.0788	39.2229
$\Delta\alpha$	33.7495	23.9514	47.2616	24.9140	21.8781	13.8163
$\Delta\alpha/\Delta\alpha(C_6H_6)$	1.000	0.710	1.400	0.738	0.648	0.409

[a] Polarizabilities are given in atomic units: 1 au $= e^2a_0^2/E_h = 1.648\,57 \times 10^{-43}$ F m^2. [b] As in Table 2.

(computed 33.7) for benzene,[42] 27.4 (computed 24.9) for *s*-triazine,[41] and 17.6 (computed 21.9) for borazine.[40]

The "aromaticity scale" obtained from the ratios $\alpha_\perp/\alpha_\perp(C_6H_6)$ for the π electrons is similar to that obtained from the magnetic susceptibilities, with only $C_5H_5^-$ out of sequence. Other scales based on polarizability values appear to be less useful. The mean total polarizability[19] makes borazine more aromatic than *s*-triazine, in contradiction to the magnetic susceptibility scales in Table 2 and to the current density maps in Figures 4 and 5. The total polarizability anisotropy, $\Delta\alpha = \alpha_\perp - \alpha_\parallel$, retrieves the "correct" order for these two molecules,[21] but the corresponding values for the π electrons suggest that the π distribution is almost isotropically polarizable in cyclopentadienyl, borazine, and boroxine.

Conclusions

The ring-current model of π electrons in planar conjugated molecules has a long history and has become part of the language of chemistry. The model can now be checked and supplemented by *ab initio* current density maps. The maps given here for benzene and its analogues have provided new insight into the concept of aromatic character and have been used to support the use of magnetic susceptibility for the construction of an aromaticity scale for these molecules.

References and Notes

(1) Pauling, L. *J. Chem. Phys.* **1936**, *4*, 673.
(2) London, F. *J. Phys. Radium* **1937**, *8*, 397.
(3) Pople, J. A. *J. Chem. Phys.* **1956**, *24*, 1111.
(4) McWeeny, R. *Mol. Phys.* **1958**, *1*, 311.
(5) Haigh, C. W.; Mallion, R. B. *Prog. Nucl. Magn. Reson. Spectrosc.* **1980**, *13*, 303 and reference therein.
(6) Keith, T. A.; Bader, R. F. W. *Chem. Phys. Lett.* **1993**, *210*, 223.
(7) Keith, T. A.; Bader, R. F. W. *J. Chem. Phys.* **1993**, *99*, 3669.
(8) Lazzeretti, P.; Malagoli, M.; Zanasi, R. *Chem. Phys. Lett.* **1994**, *220*, 299.
(9) Coriani, S.; Lazzeretti, P.; Malagoli, M.; Zanasi, R. *Theor. Chim. Acta* **1994**, *89*, 181.
(10) Zanasi, R.; Lazzeretti, P.; Malagoli, M.; Piccinini, F. *J. Chem. Phys.* **1995**, *102*, 7150.
(11) Fowler, P. W.; Zanasi, R.; Cadioli, B.; Steiner, E. *Chem. Phys. Lett.* **1996**, *251*, 132.
(12) Kutzelnigg, W. *Isr. J. Chem.* **1980**, *19*, 193.
(13) Schindler, M.; Kutzelnigg, W. *J. Chem. Phys.* **1982**, *76*, 1919.
(14) Fleischer, U.; Kutzelnigg, W.; Lazzeretti, P.; Mühlenkamp. V. *J. Am. Chem. Soc.* **1994**, *116*, 5296.
(15) Steiner, E.; Fowler, P. W. *Int. J. Quantum Chem.* **1996**, *60*, 609.
(16) Clar, E. *Polycyclic hydrocarbons*; Academic Press: London, 1964; Vol. 1.
(17) Badger, G. M. *Aromatic character and aromaticity*; Cambridge University Press: London, 1969.
(18) Garratt, P. J. *Aromaticity*; J. Wiley and Sons Ltd.: New York, 1986.
(19) Lazzeretti, P.; Tossell, J. A. *J. Mol. Struct.: THEOCHEM* **1991**, *236*, 403.
(20) Cooper, D. L.; Wright, S. C.; Gerratt, J.; Hyams, P. A.; Raimondi, M. *J. Chem. Soc., Perkin Trans. 2* **1989**, 719.
(21) Archibong, E. F.; Thakkar, A. J. *Mol. Phys.* **1994**, *81*, 557.
(22) Minkin, V. J.; Glukhovtsev, M. N.; Simkin, B. Y. *Aromaticity and Antiaromaticity: Electronic and Structural Aspects*; J. Wiley and Sons Ltd.: New York, 1994.
(23) Schleyer, P. von R.; Freeman, P. K.; Jiao, H.; Goldfuss, B. *Angew. Chem., Int. Ed. Engl.* **1995**, *34*, 337.
(24) Schleyer, P. von R.; Jiao, H. *Pure Appl. Chem.* **1996**, *68*, 209.
(25) Dauben, H. J.; Wilson, J. R.; Laity, J. L. Diamagnetic Susceptibility Exaltation as a Criterion of Aromaticity' In *Nonbenzenoid Aromatics*; Snyder, J. P., Ed.; Academic Press: New York, 1971, Vol. II.
(26) Schleyer, P. von R.; Maerker, C.; Dransfeld, A.; Jiao, H.; van E Hommes, N. J. R. *J. Am. Chem. Soc.* **1996**, *118*, 6317.
(27) Lazzeretti, P.; Zanasi, R. *SYSMO package*; University of Modena: Italy.
(28) McWeeny, R. *Chem. Phys. Lett.* **1971**, *9*, 341.
(29) Chan, S. I.; Das, T. P. *J. Chem. Phys.* **1962**, *37*, 1527.
(30) Sadlej, A. J. *Acta Physica Pol.* **1976**, *A49*, 666.
(31) Edwards, T. G.; McWeeny, R. *Chem. Phys. Lett.* **1971**, *10*, 283.
(32) Ditchfield, R. *Mol. Phys.* **1974**, *27*, 789.
(33) Lazzeretti, P.; Malagoli, M.; Zanasi, R. *J. Mol. Struct.: THEOCHEM.* **1991**, *234*, 127.
(34) van Duijneveldt, F. B. IBM Research Report RJ945; IBM Research Lab.: San Jose, CA, 1971.
(35) Dunning, T. H. *J. Chem. Phys.* **1971**, *55*, 3958.
(36) Amos, R. D.; Rice, J. E. *The Cambridge Analytical Derivatives Package*; Cambridge, UK, 1987.
(37) Haddon, R. C. *Pure Appl. Chem.* **1982**, *54*, 1129.
(38) Boyd, R. J.; Choi, S. C.; Hale, C. C. *Chem. Phys. Lett.* **1984**, *112*, 136.
(39) Černušák, I.; Fowler, P. W.; Steiner, E. *Mol. Phys.*, in press.
(40) Dennis, G. R.; Ritchie, G. L. D. *J. Phys. Chem.* **1993**, *97*, 8403.
(41) Blanch, E. W.; Dennis, G. R.; Ritchie, G. L. D.; Wormell, P. *J. Mol. Struct.:* **1991**, *248*, 201.
(42) Alms, G. R.; Burnham, A. K.; Flygare, W. H. *J. Chem. Phys.* **1975**, *63*, 3321.
(43) Hough, W. V.; Schaeffer, G. W.; Dzurus, M.; Stewart, A. C. *J. Am. Chem. Soc.* **1955**, *77*, 864.